Seismic tomography in Monte Sinni (Sardinia, Italy) coal mine

G. Rossi[1], G. Sardu[2], E. Del Negro[1], D. Sorgo[1], D. Nieto[1] and P. Podda[2]

[1] *Istituto Nazionale di Oceanografia e di Geofisica Sperimentale - OGS, Trieste, Italy*
[2] *Carbosulcis S.p.A., Carbonia, Italy*

(Received: January 29, 2009; accepted: May 22, 2009)

ABSTRACT Thanks to new "clean coal technologies", there is a renewed interest in coal and its exploitation: hence, to better evaluate a region's potentiality, and the difficulties of coal extraction, it is important to define geometry, setting and thickness of the coal seams within the embedding rocks in detail. Geophysical methods, and in particular seismic tomography across the tunnels, may provide the requested information. This paper presents the results of a seismic tomographic survey done in 2006 in the Monte Sinni mine, SW Sardinia, Italy. The tomographic velocity field obtained is compared with the coal-lithologies thickness after coal extraction. We conclude that there is an inverse correlation between seismic velocity and amount of coal, which confirms the validity of the tomographic approach in such field, and encourages to further optimize the acquisition and analysis procedures to gain a greater understanding of the mineralized seam setting and of its lateral variations.

1. Introduction

Following the climb in crude oil prices, coal is gaining a renewed interest, for its relatively low cost, its reserves being assured for about 200 years, compared to the 50 years for gas and oil, and its presence around the world not limited, as in the case of oil and gas, to a few countries. All these reasons added to the concerns over energy security and an aversion to nuclear energy, are pushing various countries to put new coal-fired plants into operation, benefitting from the so-called "clean coal" technologies that reduce sulphur and ash emissions, while increasing power-plant efficiency. Since coal-fired power plants are also among the greatest emitters of carbon dioxide (CO_2), the new power plants should also use the carbon capture techniques (CCT), and, in particular the techniques that imply the geological storage of CO_2 (Carbon Capture and Storage or CCS). In fact, part of the coal seam can be used as possible storage sites for carbon dioxide. Carbon dioxide is adsorbed by the coal seam (usually in the unmineable, deepest parts of the coal -bearing formations) to displace methane with consequent enhanced coal-bed methane recovery, the so-called ECBM.

Hence, detailed knowledge of the geometries of the coal seams and of the sterile housing rocks, and of eventual faults and fluid saturated zones, or of voids, due to past mining activities are required for a new or renewed mining activity as well as to define a possibile CO_2 geological storage site.

Among the different geophysical methods used to map the mineralized bodies (e.g., Gochioco, 2002; Paterson, 2003), the seismic method is often considered too expensive vis-a-vis its benefits, also because the detection of the thin coal lenses within the seam may be difficult

due to the limited resolution of the seismic waves. The new perspectives that CCS offers to unmineable mines and the consequent need for time-lapse imaging of the subsoil are at the basis of new studies on the application of seismic methods applied to mining (e.g., Gritto, 2003; Yancey *et al*., 2007) added to the interesting researche done in the past on the use of guide waves and seam or channel waves as support to mining activities (Krey, 1963; Mason, 1981; Pietsch and Slusarczyk, 1992). In fact, the thin coal seams, with lower seismic velocities and higher attenuation with respect to the embedding rocks, may act as low velocity channels for the propagation of elastic waves. This means that only part of the elastic energy generated by a shot in the coal is refracted along the roof and the floor of the coal as compressional (P) and shear (S) waves, travelling with their respective velocities in the bedrock. The remaining energy is on the contrary reflected back into the seam under various angles, with different phase velocities. A system of constructive interference, called seam (or channel) wave is generated, constituted by dispersive trains of the Rayleigh or Love type, that propagate in two dimensions even for very long distances within the coal seam without radiating energy in the surrounding bedrock (Greenhalgh *et al*., 1986; Gritto, 2003). Both kinds of waves (body and channel waves) may be used to detect voids or other disturbances that can affect the velocities of the embedding rock or of the seam, and may be of importance in programming the excavation and the coal extraction. A non-invasive method, like seismic tomography, that may treat, separately or together, more than one seismic phase (e.g., Vesnaver *et al*., 1999, 2003), may be of great interest in coal mining as well as in ECBM applications. Cross-well tomography has been already successfully applied to mining, to provide an image of the rock volume between two or more wells (e.g., Pratt *et al*., 1993; Hayles *et al*., 1996; Cao and Greenhalgh, 1997; Liu *et al*., 1998). In fact, the particular case of cross-well geometry is ideal for tomographic inversion, since there is one unknown only, the velocity, while high data redundancy and angular coverage may guarantee reliable inversion results. Instead of vertical wells, the sub-horizontal tunnels extensively present in a mine may be used to place sources and receivers along the face of coal seams, obtaining good estimates of the coal properties between the source and receiver locations (Gritto, 2003).

In the spring of 2006 the Istituto Nazionale di Oceanografia e di Geofisica Sperimentale – OGS (Italy) performed a seismic survey in the Monte Sinni coal mine of the Carbosulcis S.p.A., in south-western Sardinia, Italy, to verify the feasibility of the tomographic method as a tool for the advance detection of the limits and extension of the coal lenses, and to define the parameters and the modalities for its possible extensive application for such purposes. This work presents the results of such survey.

2. The coal of the Monte Sinni mine

The Sulcis region extends from north to south from the valley of the Cixerri River to the Gulf of Palmas, opposite which are the isles of Carloforte and Sant'Antioco (Fig. 1). It has been estimated that the Sulcis Eocenic Coal Basin, that covers an area of about 1400 km^2, onshore and offshore, contains 600 Mtons of subbitumineous coal reserves. The only active mine in the area (and in Italy) is the "Miniera Monte Sinni" Coal Mining Concession in the northern part of the basin, run by Carbosulcis S.p.A., a limited company which has been managed by the Sardinian Government since 1996. The coal produced is burnt at the nearby ENEL power plant of

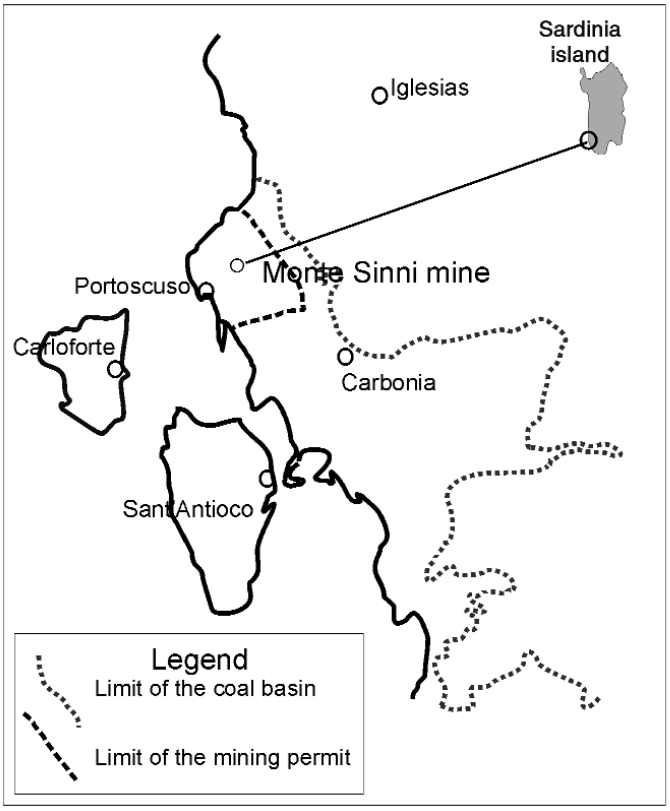

Fig. 1 - Location of the Monte Sinni mine within the Sulcis coal basin (SW Sardinia island, Italy).

Portovesme, near Portoscuso (Fig. 1).

The Sulcis coal basin has been known and exploited since the end of the 19th century, with the first mention of the presence of lignite by La Marmora (1851, 1857), Galdi (1907) and finally Taricco (1924), who for first uses the term "Produttivo" for the coal-bearing sediments, giving an estimate of its thickness in 15-40 m.

Fig. 2 shows a stratigraphic column of the formations present in the area: the coal-hosting formation is the "Produttivo", constituted by a series of limestones, and marl levels and by coal layers, of variable thickness and lateral continuity, and therefore of different economic value, alternated with sterile sedimentary layers (sandstones, silt, clay, marls) for a maximum thickness of about 80 m. It overlays the Miliolithic limestone with a trangressive contact, that presents thin coal lenses at its roof, while the passage to the overlying "Cixerri" sandstone formation is gradual. The "Produttivo" formation dips SW with a 10° inclination, reaching a depth of about 700 m in the southern part of the basin, towards the sea. The area is dominated by the extensional tectonics bound to the Alpine orogenesis that possibly reactivated Palaeozoic structures resulting in a system of horst and grabens [Fadda *et al.* (1994) and reference therein]. A series of compressive, smaller scale structures, however, as folding and minor faults, oriented from NNW-SSE to NW-SE, with variable throws dislocate the "Produttivo" and the embedding formations. The presence of these structures suggested interpreting the setting of the "Produttivo" as bound

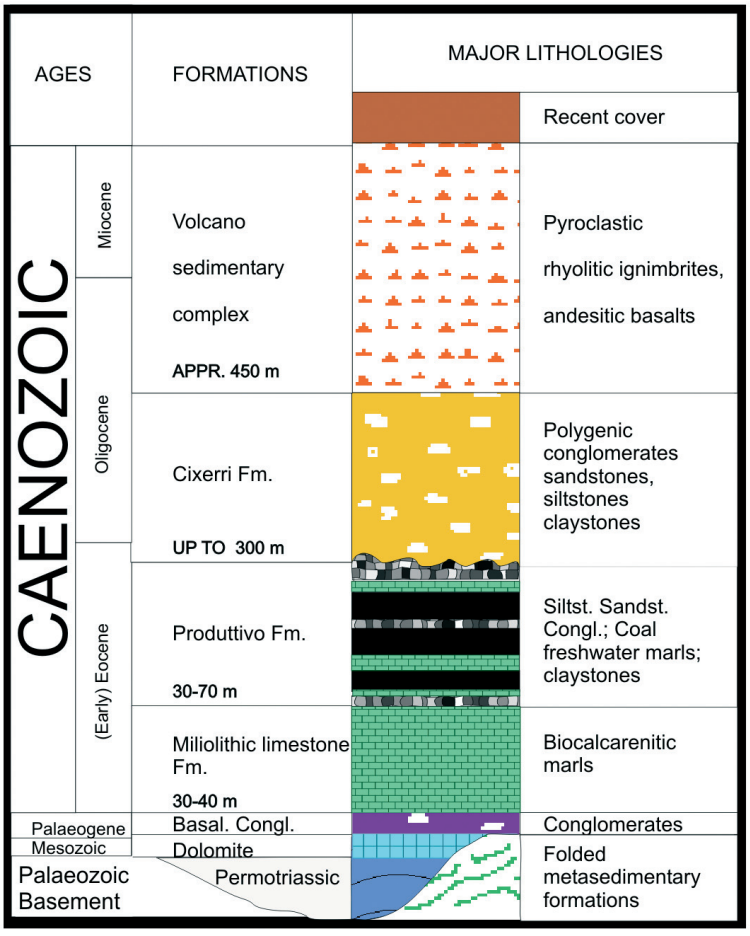

Fig. 2 - Stratigraphic column of the formations present in the area: the coal-bearing formation is the "Produttivo".

to a roll-over anticline, formed on one of the extensional structures, the Cortoghiana listric fault, to the east of the Monte Sinni mine (Fadda *et al*., 1994).

In the Monte Sinni mine, coal extraction is based on the roof support system, through hydraulic props with shearer loaders, that self advance as the face advances, while the roof behind is allowed to collapse. The cultivation is acted on panels 200 m wide and about 1 km long, starting from tunnels that are traced following the seam (Fig. 3). The complex tectonic setting described above controls the excavation of the tunnels and determines the location of the long-wall face, and therefore the panel's length.

In general the coal thickness is about 40-60% of the seam thickness. The seismic velocity contrast between the coal-bearing layers (2770 m/s) and the sterile layers (3100 m/s) is relatively low. The stratigraphic and tectonic setting of the "Produttivo" is such that, although detailed information is available from the geologic surveys along the tunnels, it is neither easy nor immediate to reconstruct or predict the coal and sterile distribution in the rock volume between them, as would be required when planning for coal extraction in order to exploit the seam to the maximum and limit the costs.

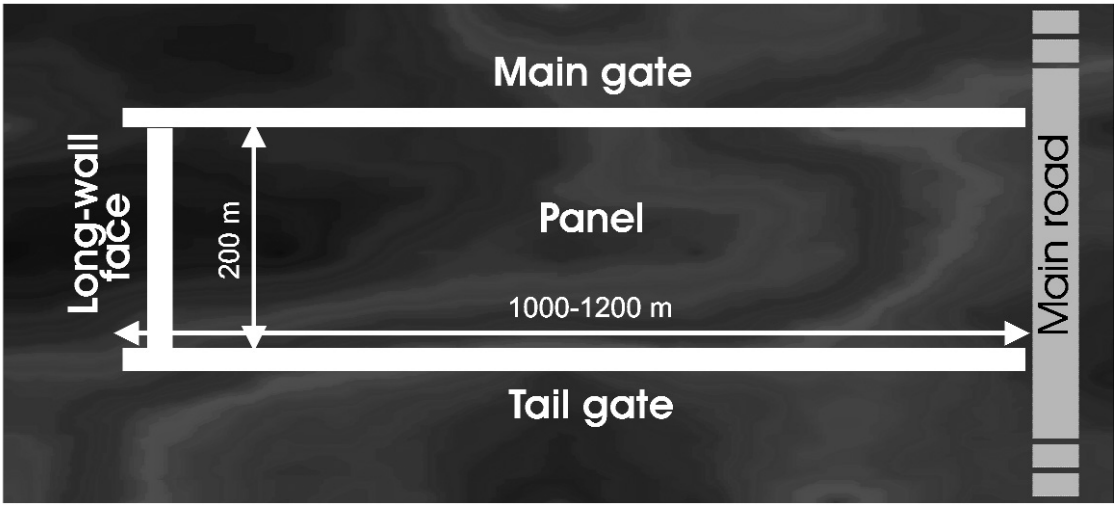

Fig. 3 - Cultivation panel: the cultivation starts from the tunnel indicated as long-wall face.

3. The survey

In order to give an answer about how the coal is distributied within the panels, a tomographic experiment was planned and carried out on one of the panels of the Monte Sinni mine, placing receivers in the tunnels, and shooting small charges in the opposite tunnel. Synthetic models have been used to test possible acquisition patterns in advance, and to optimize the duration and costs of the experiment, without loosing the resolution power. The model chosen is a schematization of the real geology, with a high-velocity meander that crosses the coal seam simulating the sterile beds within the "Produttivo" (Fig. 4a). Two possible acquisition schemes have been tested, with different intertrace and intershot distance and geometries (Figs. 4b and 4c). In particular, it was important to quantify the influence on the inversion results of a reduced source/receiver pattern, since generally, the access to one of the short sides of the panels is not possible (Fig. 4c). The results of the tomographic inversion (Figs. 4d and 4f) have been compared to the real model, obtaining the velocity residual maps (Figs. 4e and 4g respectively). It is noteworthy, that the lack of geophones on the southern side implies a lower definition of the velocity contrast between the two formations in the central part, but the general features are still recognizable.

The chosen acquisition pattern encompassed about 30 shots, spaced 30 m apart along two sides of the panel, and 110 stations, spaced 10 m apart, deployed on the opposite sides of the panel. To guarantee optimal coverage, a second acquisition was going to be done, inverting shot and receiver positions along the panel sides. However, technical problems reduced this second acquisition, and the resulting pattern is drawn in Fig. 5. The stations on the main road recorded only three of the shots. The angular coverage and data redundancy are, however, sufficient to guarantee the statistical noise reduction and good results for the tomographic inversion. After some on-site tests on the signal-to-noise ratio, small charges of 120 g of explosive were used as a source and placed into holes about 1 m deep. The sensors were 10 Hz three component geophones, deployed horizontally in the walls of the tunnels, in small holes about 10 cm deep,

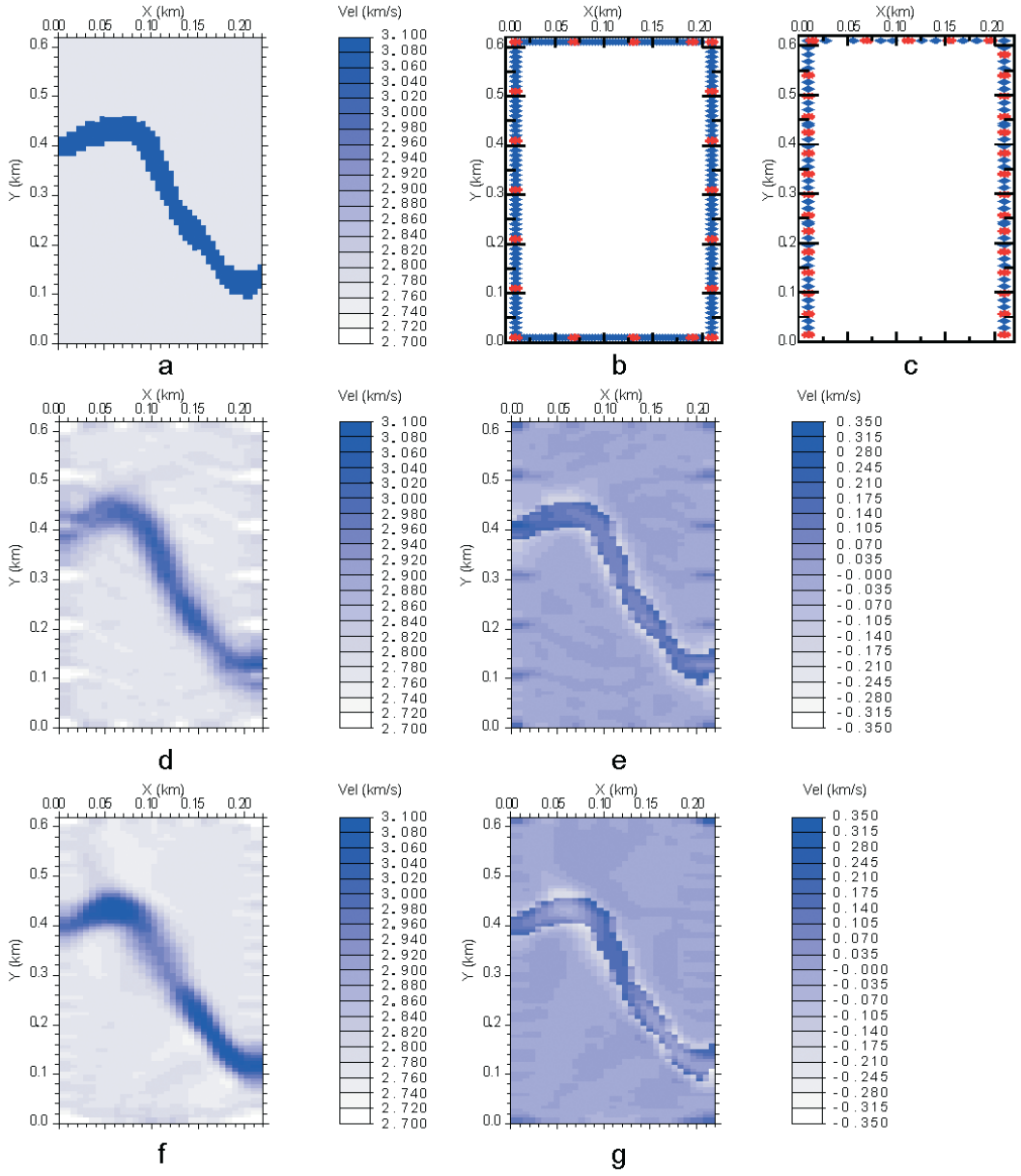

Fig. 4 - a) planar view of a synthetic model; b), c) different acquisition patterns: red stars: shots; blue rhombi: geophones; d) tomographic inversion for the acquisition shown in b; e) its misfit; f) tomographic inversion for the acquisition shown in c; g) its misfit.

depending on the alteration of the wall. The two horizontal components are N-S and E-W oriented respectively, the third component is vertical.

The time delay caused by the variable shot hole lengths may be summed up to the one caused by the use of delayed detonators, that have to be used in mines for safety reasons. The nominal delay of the used detonators is 100 ms. From the inspection of the first break of a test shot (Fig.

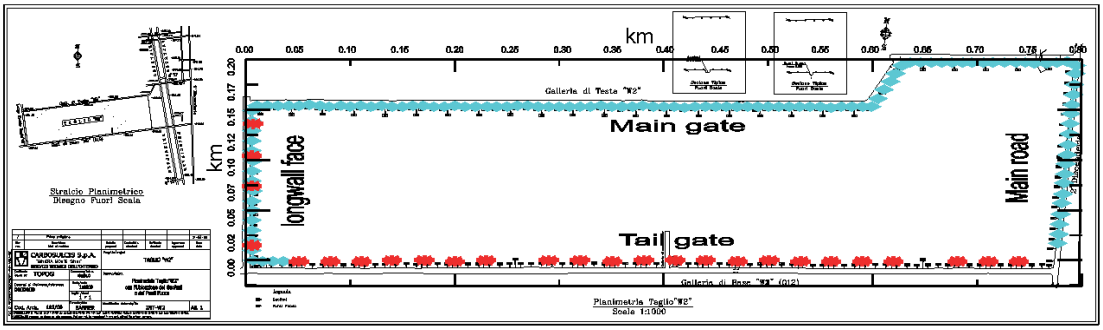

Fig. 5 - Planar view of the acquisition pattern superimposed on the map of the panel and the surrounding tunnels: red stars: shots, blue rhombi: geophones.

6) it is possible to infer a much higher delay, of about 138 ms. To verify this, the traveltimes picked for different shots were corrected for the above 138 ms delay and for other values, applied to all the shots, and the relative apparent velocities were calculated (Fig. 7). Overall at small offsets, the values are dispersed and unreliable, suggesting variable delays for each shot. This is a problem that in the future may be easily avoided by placing a geophone near the shot, to record the zero time. An iterative procedure of minimization of the time residuals overcame this problem. As a first step, the average velocity was calculated on the basis of adjacent traces, and used to calculate the arrival time at the nearest receiver with respect to each shot and use the time difference with the observed traveltime, to correct the zero time for all the traces. The applied corrections are checked through a new analysis of the apparent velocity as a function of the trace number (Fig. 8). The comparison of the values obtained at the beginning of the iterative procedure (red curve) with the ones obtained at the end of it (black curve) put in evidence how, through the

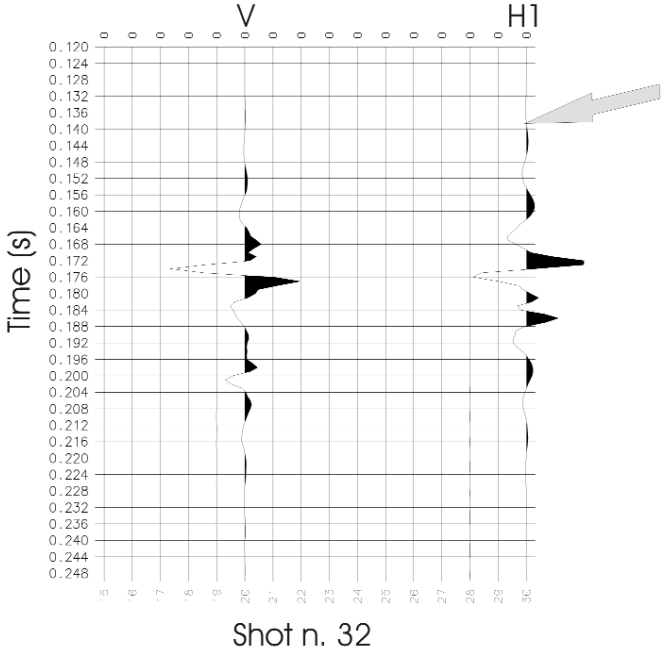

Fig. 6 - Test shot to evaluate the zero time. Two components are shown (V=vertical; H1=one of the two horizontal ones). The arrow indicates the first break, at about 138 ms.

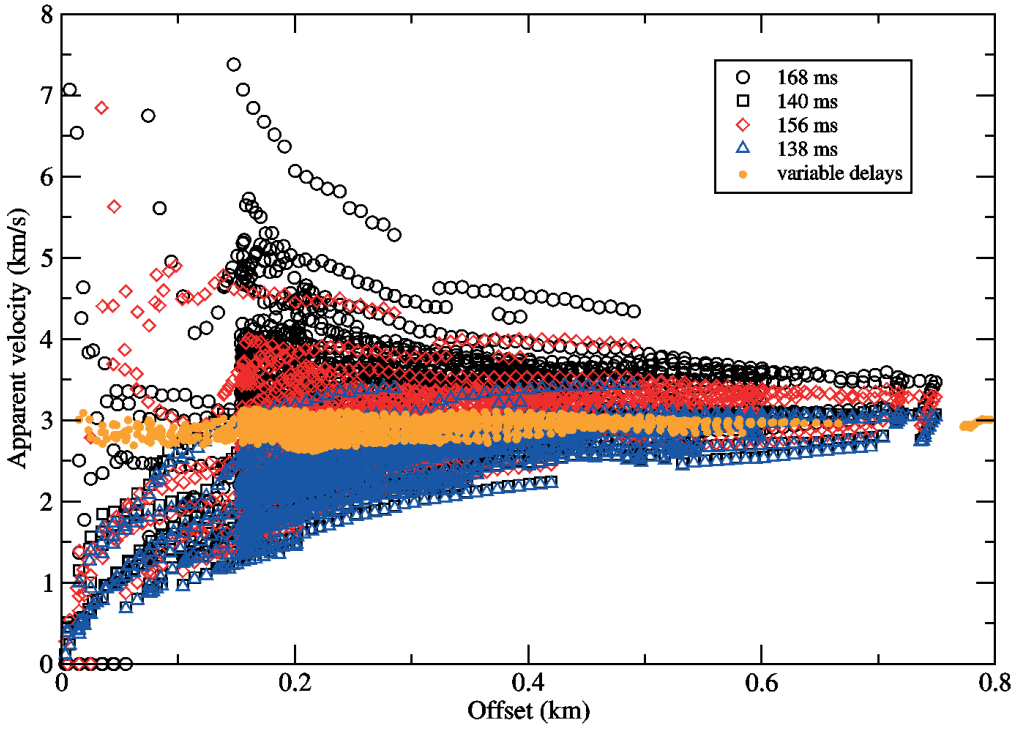

Fig. 7 - Delay minimization procedure: y-axis: apparent velocities (km/s); x-axis: offset. Comparison between the results obtained by applying constant different delays to all the shots (black circles, red rhombi, black squares and blue triangles) and variable delays, calculated for each shot (orange dots).

reduction of the errors in the effective zero-time values the dispersion in the apparent velocity values is strongly reduced. The velocity values so obtained are plausible for the rocks crossed by the seismic rays, also for the nearest offset, as may be seen in Fig. 7 (orange dots).

Fig. 9 shows the traces of a shot gather of one of the three components. An evident low - frequency component, probably due to environmental noise, is present (left). After the band-pass filtering (right), the first arrivals are more evident, as well as other phases, that may be related to the presence of seam waves (Krey, 1963; Mason, 1981; Pietsch and Slusarczyk, 1992) which will be the object of future analyses. The relative spectra are shown at the bottom, to show the frequency content of the different phases.

4. The tomographic analysis

We rotated the two horizontal components according to the azimuth of each source-receiver couple, obtaining the radial and the transverse components of the wave field. We picked the first arrivals on the radial component that in the acquisition geometry described above are supposed to record the compressional waves. Fig. 10 reports the traces of the relative rays. Notwithstanding the reduced acquisition pattern, the panel is well covered by the seismic rays, which implies a

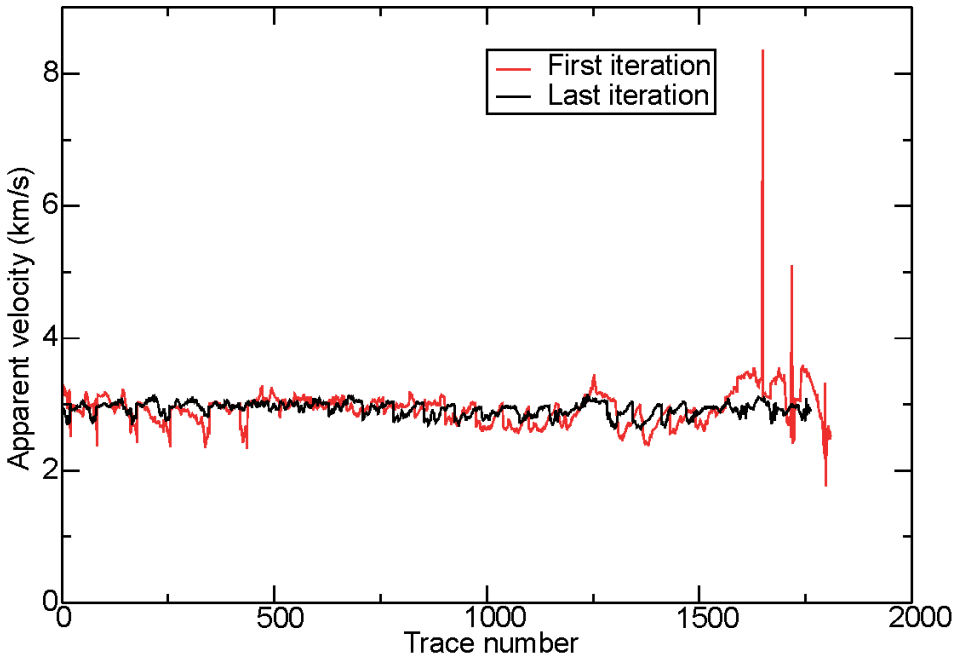

Fig. 8 - Minimization procedure results: y-axis: apparent velocities (km/s); x-axis: trace number. Red curve: first step of the iterative procedure; black curve: last iteration.

reliable successive tomographic inversion of the data. It is however evident than there is a lack of coverage on the right, due to the fact that the stations along the main road recorded only a few of the shots. Some coverage interruption along the tail gate is due to a too low signal-to-noise ratio that did not enable a correct picking of the data.

To minimize the consequences of this, as well as the possible coupling effects of geophones with the galleries walls, we chose a coarse irregular grid, adapted on the ray coverage, using the Voronoi polygons (Böhm and Vesnaver, 1999) (Fig. 11). This results in about 8 pixels in a N-S direction, and about 40-50 in a E-W direction, the grid being coarser along the less covered tunnel walls, and finer in the well covered central part of the panel. At the end of the tomographic loop, to guarantee the high resolution requested, without loosing in reliability, we applied the staggered grid procedure to the adapted one (Vesnaver and Böhm, 2000). We performed three shifts of 5 m in both x and y directions, and we averaged the relative tomographic results, obtaining a grid with higher resolution with respect to the base grid (24 pixels in N-S direction, 150 in E-W direction). In Fig. 12, it is possible to compare the ray distribution we get at the end of the grid through the adapting and staggering procedure with the one of the corresponding high resolution regular grid (Fig. 12b). A better measure of the inversion reliability is given by the null space energy that depends not only upon the ray number, but upon their relative distribution, and relation with the grid geometry. A high number of subparallel rays implies a linear dependency between the rays, and hence a high null space energy (Vesnaver, 1994). The null space energy obtained at the end of the staggering procedure and the one of the high resolution grid may be compared in Figs. 13a

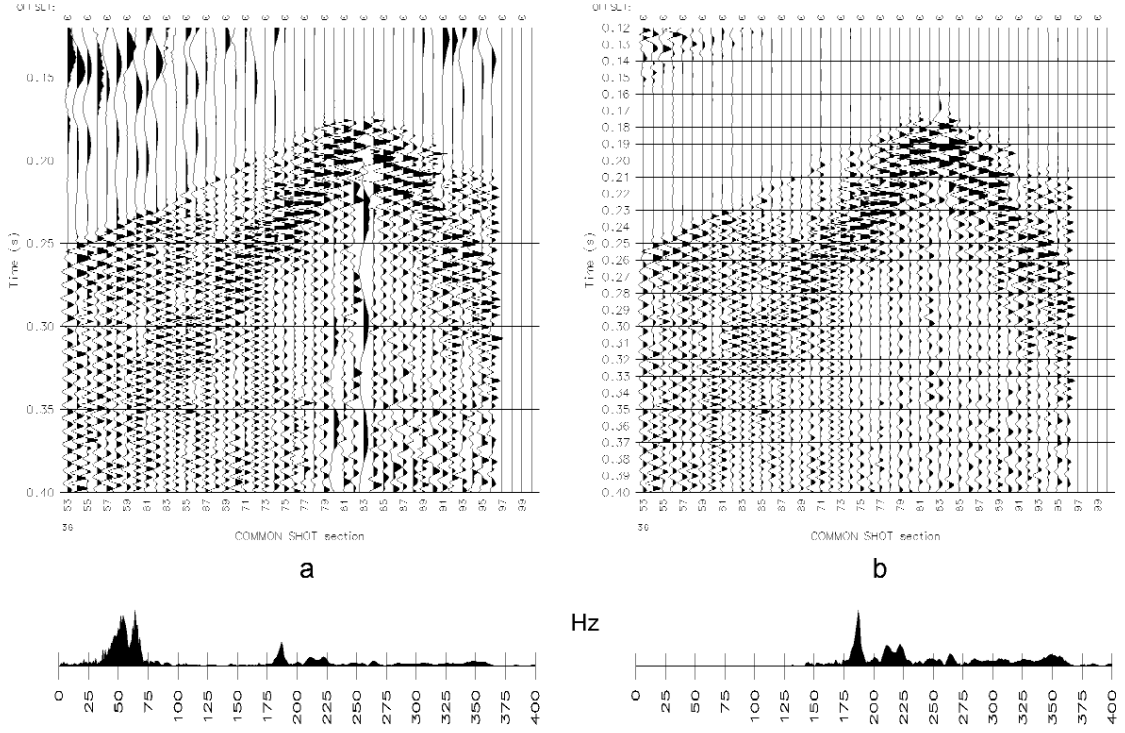

Fig. 9 - Shot 36: a) seismic traces; b) the same data after a band pass filtering; c) amplitude spectrum of one trace of a; d) amplitude spectrum of one trace of b.

and 13b, respectively. It may be seen how the staggering grid procedure allows us to obtain a better ray distribution, with a less marked acquisition footprint. The number of rays that cross the large pixels of the base grid, that is laterally shifted and averaged in the staggering loop, is higher than it would be on the small pixels of the final grid. As said, this reflects on the null space energy,

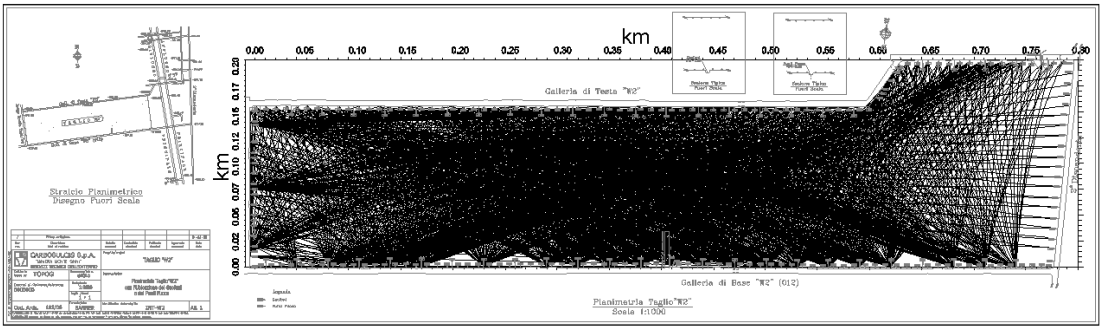

Fig. 10 - Planar view of the seismic rays corresponding to the picked compressional direct arrivals, superimposed on the panel and tunnels map

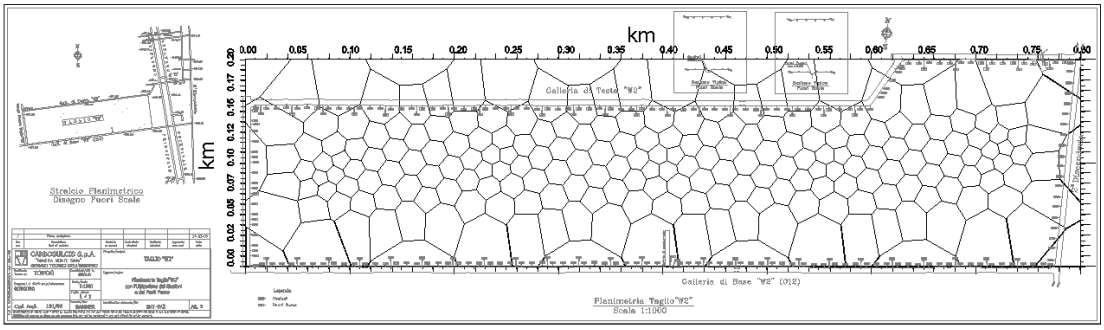

Fig. 11 - Planar view of adaptive grid, based on the ray-coverage of Fig. 10, superimposed on the panel and tunnels map.

that results much smaller, with higher values limited to small regions, so that the information on seismic velocity is better constrained.

For the velocity inversion, we used the inversion procedure described in detail by Vesnaver *et al*. (1999) that consists in a modified version of the minimum time ray tracing developed by Böhm *et al*. (1999) and an iterative procedure for the inversion, based on the Simultaneous Iterative Reconstruction Technique (SIRT) algorithm. The initial model has a constant velocity of 3000 m/s, except in the pixels not crossed by the rays, within the tunnels, to which air velocity (330 m/s) is

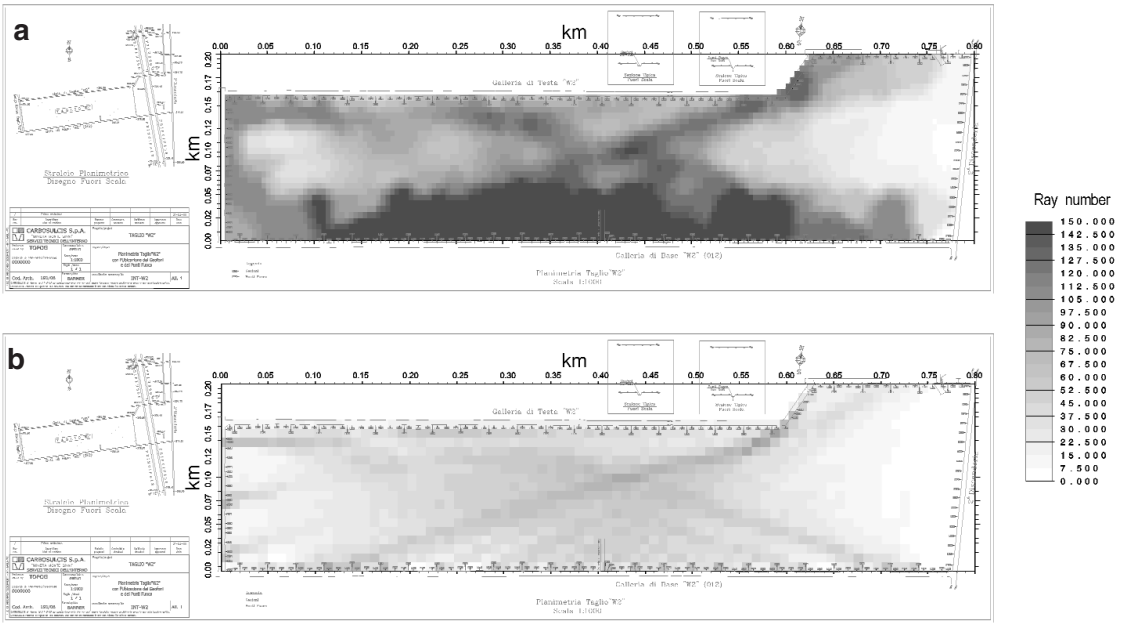

Fig. 12 - Planar view of the seismic ray distribution, as resulting at the end of the adaptive and staggering grid procedure (a) and on the corresponding fine regular grid (b).

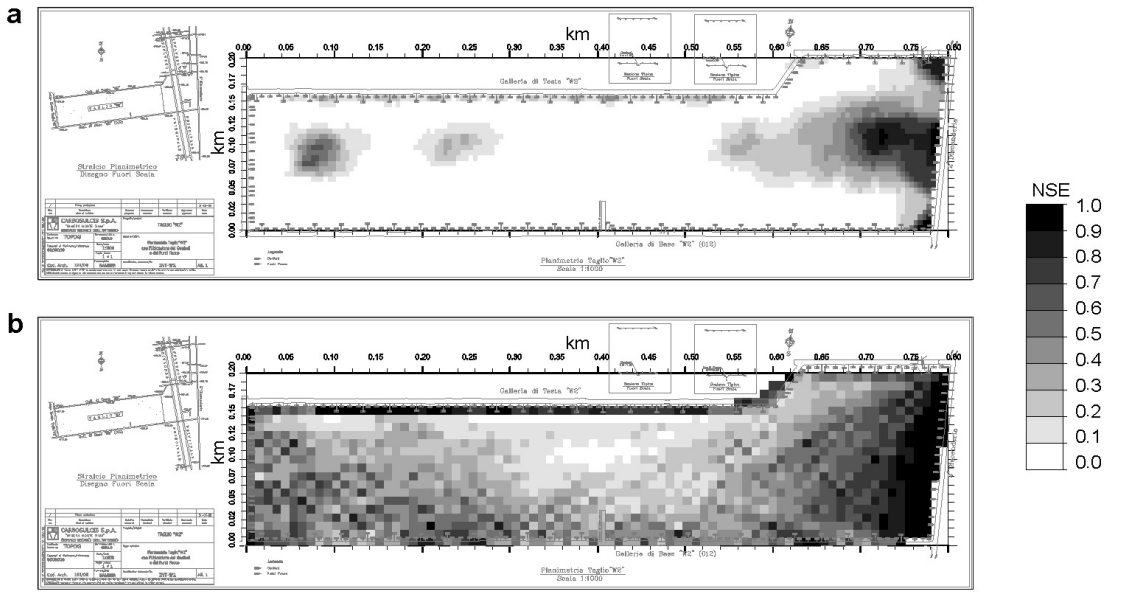

Fig. 13 - Planar view of the null space energy as resulting at the end of the adaptive and staggering grid procedure (a) and on the corresponding fine regular grid (b).

given. The importance of the initial model however is inversely proportional to the ray-coverage and reliability of the inversion. The higher the latter, the more independent from the initial model is the solution. We did two iterations with the SIRT method, and 20 iterations for each ray provide the correct ray-tracing, with time residuals around 0.003 s. Fig. 14 shows the results of the tomographic inversion. The areas where the tomographic results are less reliable, due to the poor coverage, are masked by a black and white colour scale, based on the null space energy values of Fig. 13a.

The velocity values obtained from the direct arrivals inversion are in agreement with the

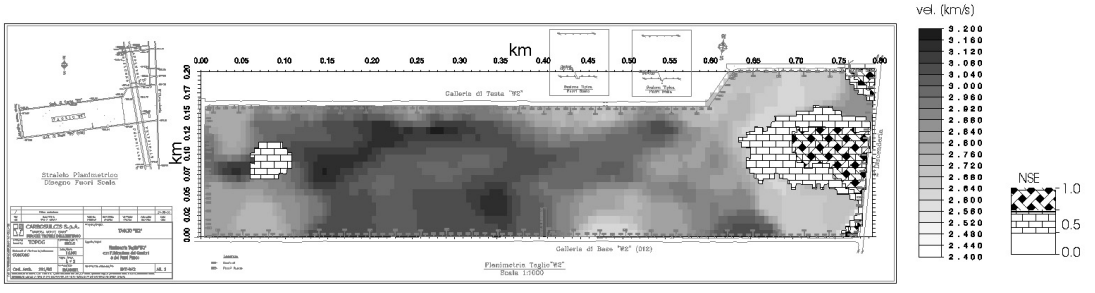

Fig. 14 - Planar view of the resulting velocity field: the reliable low areas are masked, following the null space values of Fig. 13a.

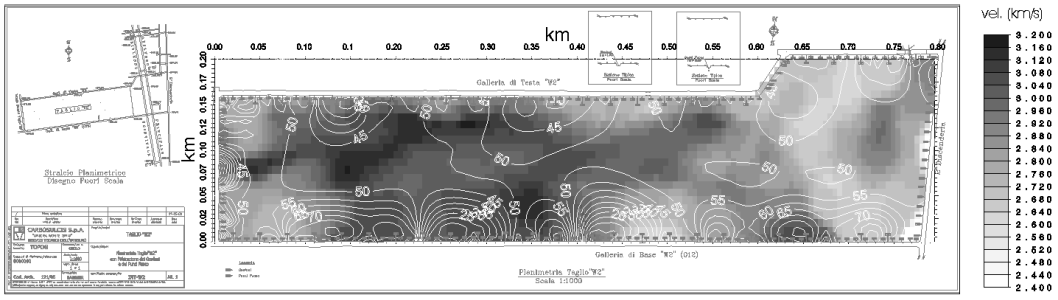

Fig. 15 - Planar view of the velocity field superimposed by the isolines deriving from the extrapolation of the remainder of the panel of the coal percentage observed on the tunnel walls.

available information, according to which values of about 2.77 km/s should be of the coal bodies (white-to-pale grey in the scale of Fig. 14) while values above 3 km/s should belong to the sterile formations (limestones and sandstones) (dark grey-to-black in Fig. 14).

5. Discussion

The correlation between seismic velocity values and coal distribution is confirmed by the comparison with the geological sections traced along the walls of the tunnels, and with the coal percentage calculated on the basis of them. This percentage has been extrapolated from the remaining parts of the panel and contoured: Fig. 15 shows the relative isolines (white) superimposed on the velocity field of Fig. 14. Noteworthy, is a certain correlation between low velocities and higher coal percentage, and vice versa.

To have however a more rigorous evaluation of the correlation of the velocity and the coal amount, we calculated the correlation coefficient on the same points along the tunnels, spaced 10 m apart. We averaged the velocity values on cells 10 m wide in the direction parallel to the tunnels, and 25 in the direction normal to them. More than 50% of the correlation coefficient values lay within the interval between -0.55 and -0.6, and the 90% of them within the interval between -0.45 and -0.7, to confirm a certain negative correlation: high values of the seismic velocities are observed in correspondence of low coal percentages, and vice versa. In the months following the tomographic survey, the coal excavation was done and completed, so that it was possible to have a better and more complete comparison of the seismic velocity values and the real coal amount extracted from the panel, or better, the coal lithologies' thickness (Fig. 16). We used an inverse scale for the velocities and coal thickness in order to facilitate the visual comparison.

Notwithstanding the fact that the tomographic velocities give average information, the inverse correlation between seismic velocities and coal amount is confirmed. The major discrepancy is observed near the tail tunnel, at x=500, where low signal to noise ratio caused a lack of coverage.

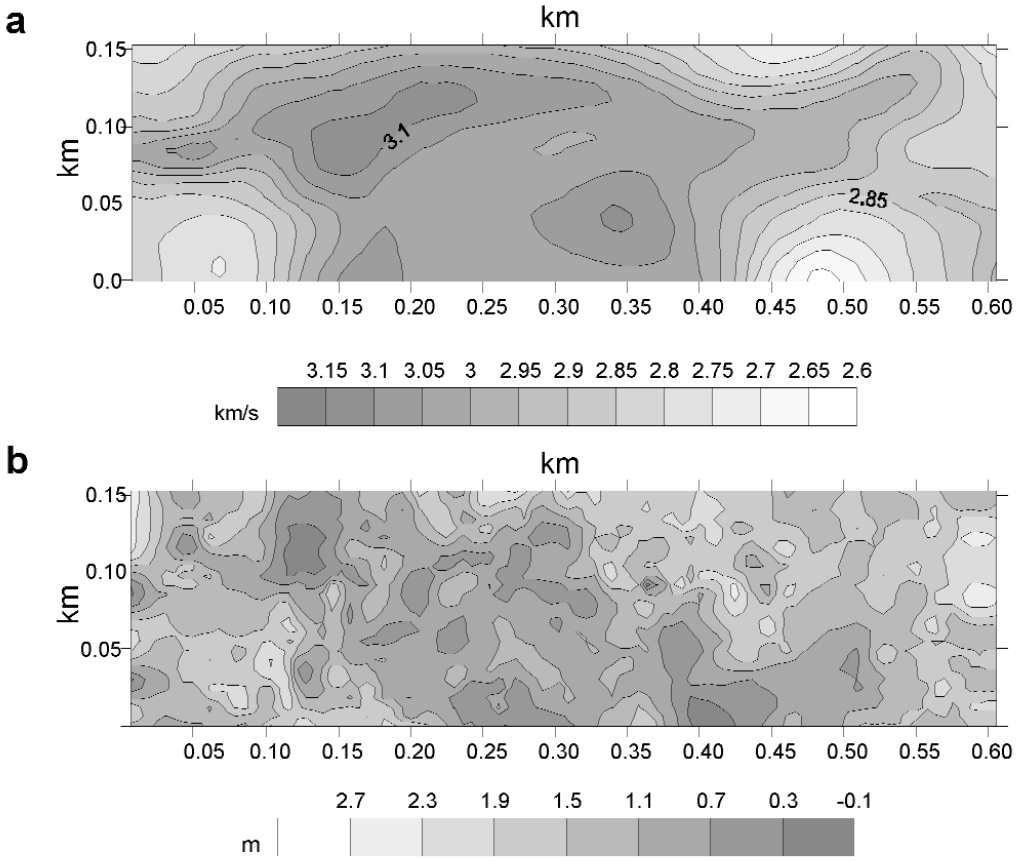

Fig. 16 - Planar view of the tomographic velocity field (a); and the interpolated coal thickness observed in the panel after its excavation (b).

6. Conclusions

The results of the tomographic inversion of the data acquired in the Monte Sinni mine in spring 2006 are promising and encouraged the continuation of the tests. During summer 2007, a new acquisition was done while bearing in mind past experience: source and receiver interval is half (15 and 5 m, respectively), zero time has been recorded, and the acquisition pattern guaranteed an optimal coverage. The resulting tomographic field, with a higher resolution with respect to the one here presented here, is presently being compared with the coal thickness and percentage data from the on-going excavation, but the results achieved until now are good, confirming the high capability of tomographic inversion in giving a good estimate of coal distribution between the tunnels, through the inverse correlation of seismic velocities with coal thickness. The results presented constitute also a starting point for the development of new research aimed at exploiting the whole wave field recorded, including in the tomographic inversion of other phases, as seam waves, leading to a more complete comprehension of the

mineralized seam setting and its lateral variations.

Acknowledgements. This paper was presented at the 27th GNGTS 2008 conference. We thank the Carbosulcis S.p.A. for the permission to publish these results, as well as all its whole personnel, for the enthusiastic and precious help they gave us during the acquisition. Thanks also go to Giuliano Brancolini, Gualtiero Böhm and Flavio Accaino for their constructive discussions, advice and help in the different phases of the project. We are also grateful to both reviewers for their useful and detailed comments on the manuscript.

REFERENCES

Böhm G. and Vesnaver A.; 1999: *In quest of the grid.* Geophysics, **64**, 1116-1125.

Böhm G., Rossi G. and Vesnaver A.; 1999: *Minimum time ray-tracing for 3-D irregular grids.* J. Seism. Explor., **8**, 117-131.

Cao S. and Greenhalgh S.; 1997: *Crosswell seismic tomography delineation of mineralization in hard-rock environment.* Geophysical Prospecting, **45**, 449-460.

Fadda A., Ottelli L. and Perna G.; 1994: *Il bacino carbonifero del Sulcis: Geologia, idrologia, miniere.* Cagliari, 144 pp.

Galdi B.; 1907: *Notizie sui giacimenti di lignite dell'Iglesiente.* Pubbl. Corpo Reale Miniere, Roma, 55 pp.

Gochioco L.M.; 2002: *Recent role of geophysics in US coal and CBM development.* The Leading Edge, **21**, 452-455.

Greenhalgh S.A., Burns D. and Mason I.; 1986: *A cross-hole and face-to-borehole in-seam seismic experiment at Invincible Colliery, Australia.* Geophysical Prospecting, **34**, 30-55.

Gritto R.; 2003: *Subsurface void detection using seismic tomographic imaging.* LBNL 53227, Lawrence Berkeley National Laboratory (ed), Berkeley, USA, 10 pp.

Hayles J.G., Serzu M.H., Lodha G.S. and Read R.S.; 1996: *Cross-hole seismic tomography surveys for the mine-by experiment*. In: Society of Exploration Geophysicists (ed), Proc. of 66th Meeting, Society of Exploration Geophysicists, SEG Expanded Abstracts, **15**, Tulsa, pp. 904-907.

Krey T.C.; 1963: *Channel waves as a tool of applied geophysics in coal mining.* Geophysics, **28**, 701-714.

La Marmora A.; 1851: *Due parole sulla classificazione geologica del combustibile di Gonnesa e di altri luoghi del Sulcis in Sardegna.* Timon Tip., Cagliari, 19 pp.

La Marmora A.; 1857: *Voyage en Sardaigne.* Troisiéme partie. Description géologique et paléontologique, 2 volumes, Frères Bocca, Impr. Royale, Librairies du Roi, Torino, 781 pp.

Liu L., Lane J.W. and Quan Y.; 1998: *Radar attenuation tomography using the centroid frequency downshift method.* J. Appl. Geophys., **40**, 105-116.

Mason I.; 1981: *Algebraic reconstruction of a two-dimensional velocity inhomogeneity in the High Hazle seam of Thoresby colliery.* Geophysics, **46**, 298-308.

Paterson N.M.; 2003: *Geophysical development and mine discoveries in the 20th century.* The Leading Edge, **22**, 558-561.

Pietsch K. and Slusarczyk R.; 1992: T*he application of high resolution seismic in Polish coal mining.* Geophysics, **57**, 171–180.

Pratt R.G., McGaughey W.J. and Chapman C.H.; 1993: *Anisotropic velocity tomography: a case study in a near surface rock mass.* Geophysics, **58,** 1748-1763.

Taricco M.; 1924: *Il bacino lignitifero di Gonnesa (Provincia di Cagliari).* Boll. R. Uff. Geol. Ital., **49** (9), 1-14.

Vesnaver A.; 1994: *Towards the uniqueness of tomographic inversion solutions.* Journal of Seismic Exploration, **3,** 323-334.

Vesnaver A. and Böhm G.; 2000: *Staggered or adapted grids for seismic tomography?* The Leading Edge, **19**, 944-950.

Vesnaver A., Böhm G., Madrussani G., Petersen S. and Rossi G.; 1999: *Tomographic imaging by reflected and refracted arrivals at the North Sea.* Geophysics, **64**, 1852–1862.

Vesnaver A., Accaino F., Böhm G., Madrussani G., Pajchel J., Rossi G. and Dal Moro G.; 2003: *Time-lapse tomography.* Geophysics, **68**, 815-823.

Yancey D.J., Imhof M.G., Feddock J.E. and Gresham T.; 2007: *Analysis and application of coal-seam seismic waves for detecting abandoned mines.* Geophysics, **72**, M7-M15.

Corresponding author: Giuliana Rossi
Istituto Nazionale di Oceanografia e di Geofisica Sperimentale
Dipartimento di Geofisica della Litosfera
Borgo Grotta Gigante 42/c, 34010 Sgonico (Trieste), Italy
phone: +39 040 2140347; fax: +39 040 327307; e-mail: grossi@inogs.it